Solar Energy 149 (2017) 132–144

Contents lists available at ScienceDirect

Solar Energy

journal homepage: www.elsevier.com/locate/solener

Design and construction of a charge controller for stand-alone PV/battery hybrid system by using a new control strategy and power management

Amin Mirzaei [a,*], Majid Forooghi [a], Ali Asghar Ghadimi [a], Amir Hossein Abolmasoumi [a], Mohammad Reza Riahi [b]

[a] Department of Electrical Engineering, Faculty of Engineering, Arak University, Arak, Iran
[b] Sharif University of Technology, Tehran, Iran

ARTICLE INFO

Article history:
Received 18 December 2016
Received in revised form 1 March 2017
Accepted 15 March 2017

Keywords:
State of charge
MPPT
DC-DC converter
Photovoltaic

ABSTRACT

In this paper, a new control strategy and power management for a stand-alone PV/battery hybrid power system has been suggested. The solar cell arrays provide energy in the steady-state and the battery provides energy in transient states. Here, a charge controller system based on the MPP tracking technology, suitable for using in the islanded micro grid that contains a solar panel and a battery is designed. The charge controller includes a unidirectional DC-DC converter as an interface circuit between the solar panel and the DC bus, a bidirectional DC-DC converter as an interface circuit between the battery and the DC bus with a control system and power management in different states of irradiance and state of charge (SOC). A 200-W prototype system is designed and simulated in MATLAB/Simulink software. Also, a microcontroller DSP TMS320F2812 is applied to construct the charge controller circuit. The simulation and experimental results are showing better performance of the proposed charge controller compared with previous examples.

1. Introduction

Solar energy in the recent years in all countries of the world due to excessive energy crisis and environmental pollution is considered seriously. Photovoltaic systems which convert solar energy directly to electricity, now are one of the most common resources of electrical energy. They can be used in grid-connected mode to support the network or in stand-alone mode to supply some islanded loads. In stand-alone mode, the PV independently cannot be enough for supplying loads because weather conditions (such as clouds and fog) have a significant impact on the solar energy received by a PV array. So, there is a need for energy storage systems like batteries. Since both the PV array and the batteries are DC sources, they are connected to the DC bus via DC-DC converters.

There are several important issues in a stand-alone PV/battery system. Efficiency, controllability, MPPT capability, proper protection scheme, system weight, battery lifetime, battery charge and discharge pattern, system on/off mode, system cost, output voltage quality, etc. these features are affected by the type and configuration of the DC-DC converters, size of batteries and PV arrays, control strategy, MPPT algorithm, and energy management system. So, proper selection and adjustment of aforementioned parameters is the most vital task of PV system designers, this system is titled PV charge controller (Mojallizadeh et al., 2016; Fathabadi, 2016; Fernão Pires et al., 2016; Karami et al., 2012; Lu and Nguyen, 2012; Masheleni and Carelse, 1997).

In prior research, several aspects of the PV charge controllers are considered. In Zhiling and Xinbo (2009) a control strategy and power management for a stand-alone PV power system is proposed. The working situations of the proposed control strategy are divided into four modes that they can happen in eight conditions. In this reference three different working situations for unidirectional DC-DC converter connected to a PV is mentioned (MPP tracking (MPPT) mode, constant voltage mode (CV) and off mode), which each of these modes makes the PV voltage remains constant. In the management system, the PV voltage is considered as an independent variable that determines the operation mode of the converter. But, this is not practical since the PV voltage must be controlled and it is a dependent variable. So, it cannot independently determine the operation mode of the system. In Mahmood et al. (2015) a control strategy to achieve decentralized power

* Corresponding author.
E-mail addresses: a-mirzaee@araku.ac.ir (A. Mirzaei), majidforooghi@gmail.com (M. Forooghi), a-ghadimi@araku.ac.ir (A.A. Ghadimi), a-abolmasoumi@araku.ac.ir (A.H. Abolmasoumi), riahi.mohammadr@gmail.com (M.R. Riahi).

http://dx.doi.org/10.1016/j.solener.2017.03.046
0038-092X/

management for a PV/battery hybrid unit in a controlled islanded micro-grid is suggested. Contrary to the usual methods that consider the PV unit as a current source, in the proposed strategy the PV unit controlled as a voltage source. Also in Mahmood et al. (2012), a power management strategy for a battery/PV hybrid system is investigated.

In Mahmood et al. (2015, 2012) there is no plan for battery excessive discharge mode. In Nguyen et al. (2013) a comprehensive design approach in details for a fast and low-cost solar charger with the rooftop PV array of the vehicle is provided. A PV array as a power source is used to charge the battery. Hence, a DC-DC converter is applied to charge the battery. According to available energy of the PV array and the SOC of the battery, the converter can operate in one of three charge modes; MPPT charge, constant current charge (CC) and CV charge. In Nguyen et al. (2013) how to connect the battery to the load has not been investigated. In fact, excessive discharge mode in this reference is also not considered. In Hasan et al. (2009) a new control strategy that focuses on controlling a battery management system (BMS) for using with PV is presented. The strategy presented in this reference has unnecessary complication and unwanted interruptions of the battery from the circuit. For example, the mode that the SOC of the battery is more than 90% and the load power is more than PV power, or when the SOC of the battery is less than 40% and simultaneously the load power is less than PV power does not happen practically. However, the strategy has been mentioned and causes unnecessary complications. Also, instead of off modes of the circuit, better solutions can be found. In Zhenhua (2006) a power management for PV/fuel cell/battery hybrid power systems is designed. In the proposed strategy, the battery charging current limitation is not considered and the battery is connected directly to the DC bus. The PV control strategy would only prevent overcharging but protect the battery from over discharging in the control strategy has not been considered. In Chiang et al. (2009) modeling and controller design of the PV charger system with SEPIC converter is presented. In this reference the battery is connected directly to the DC bus as same as Zhenhua (2006). In Zhenhua and Dougal (2004) a new control algorithm for stand-alone PV power systems are suggested. This system has a very complex control algorithm, which contains five operating modes that are activated by ten occurrences of the conditions. In this structure, the battery is connected directly to the DC bus too. In Tofighi and Kalantar (2011) a control strategy for stand-alone PV/battery hybrid system is proposed. Power management strategy is done via passivity-based control. This strategy only offers the reference values for PV and battery and there is no debate about how to apply the powers and the fact that what happens if the reference powers were more than the maximum power of the PV and battery.

In this paper, a power management strategy that includes five operating modes for a hybrid photovoltaic battery system is proposed. The proposed strategy can manage the DC-DC converter performance and the load status, despite the SOC functional limitations, battery charging current and the PV output power. A 200 W prototype system is used to show the performance of the energy management strategy.

The rest of the paper is so organized that describe the proposed system. In the Section 2, the review on the system structure and power management strategy is provided. Then, in the Section 3, the modeling methods of the system elements and controllers are discussed. The simulation and experimental results are presented in the next section and the conclusion is done in the last part.

2. The system structure and the energy management strategy

To employ batteries with solar systems, two types of structures have been proposed in the literatures. In the first structure, battery is connected directly to the DC bus. So, the DC bus voltage is determined by the battery (Nguyen et al., 2013; Zhenhua, 2006; Chiang et al., 2009; Zhenhua and Dougal, 2004; Mirzaei et al., 2011a). For example, one application of this structure is in uninterruptible power supply (UPS) based on PV (Mahmood et al., 2012). In many such cases, the PV array output power is controlled so that the (SOC) of the battery is less than the maximum. Consequently, the battery charging current does not exceed the maximum capacity of the battery charging current. In these systems, the occurrence of a short circuit in the DC bus causes the serious damage to the battery and the battery discharge current is not controlled. Also, the number of batteries must be such as to reach the required voltage for the DC bus, and it reduces the matching flexibility of system components and reduces reliability. Another structure is shown in Fig. 1. In this structure, the battery is connected to the DC bus by a bi-directional DC-DC converter (Zhiling and Xinbo, 2009; Mahmood et al., 2015, 2012; Hasan et al., 2009; Tofighi and Kalantar, 2011; Mirzaei et al., 2011b).

This arrangement provides greater flexibility in the choice of battery rated voltage. Battery discharge current that feeds the load is controlled and in case of short circuit in the DC bus, battery is protected. In this structure, the DC link voltage is set by the bidirectional converter. To facilitate the MPPT operation, unidirectional converter is controlled. This control is done by regulating

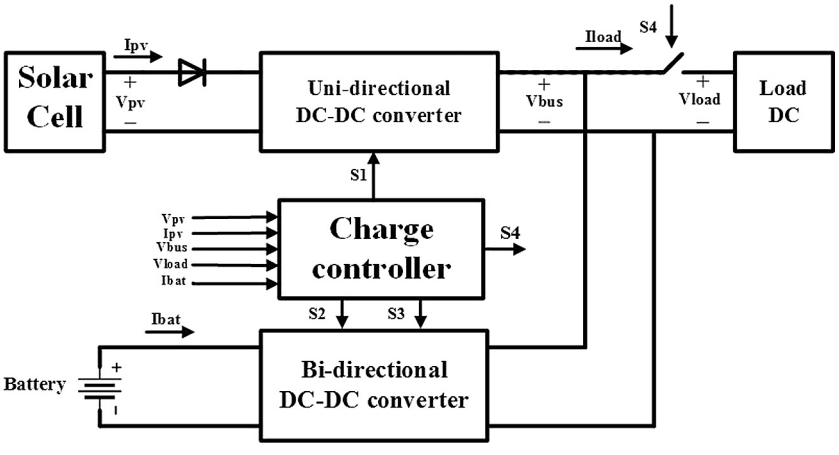

Fig. 1. The structure of PV/battery hybrid system (Mahmood et al., 2012).

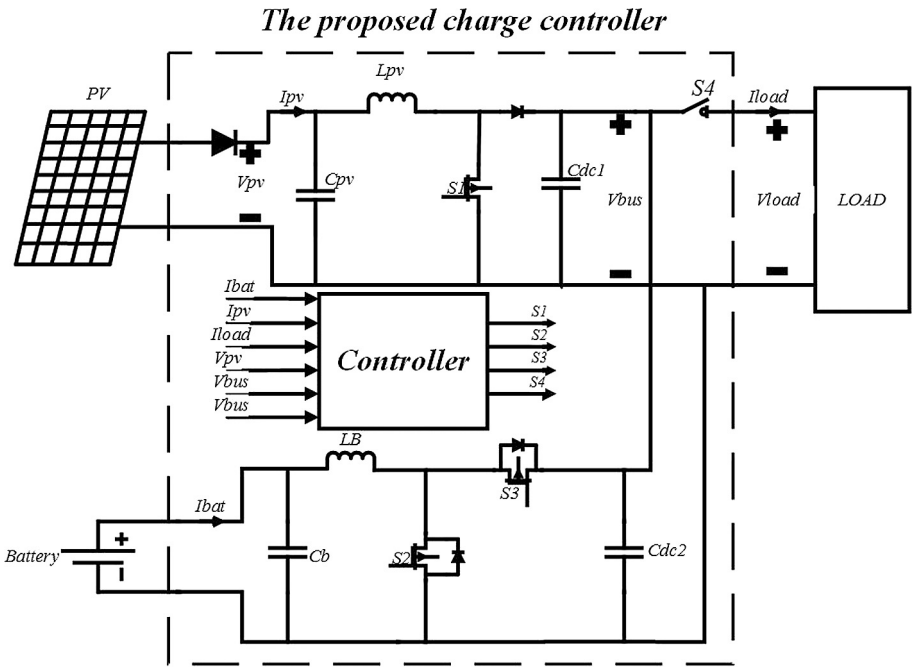

Fig. 2. The structure of the proposed charge controller.

the voltage at the converter input terminal for PV and works during normal operation at the MPP.

In the proposed stand-alone PV/battery hybrid system, a new power management strategy is employed. Two DC-DC converter as interface circuits between PV array, the battery bank and a DC link are used. The proposed control strategy, manage the power flow between the PV array, battery and load by converters and maintain the power balance in the system. It also enables the battery to support the PV array. A multi-loop control strategy is used to control the converter that is concerned with the limitation of the battery excessive charge or discharge (the limitation of battery capacity) and limitation of battery charge current. The structure of the proposed PV/battery hybrid system is shown in Fig. 2.

The proposed system as shown in Fig. 2 includes the following sections. Then, each of these sections are explained. These sections are: the solar panel, unidirectional converter for the PV array, bidirectional converter for the battery, battery, load, control system and energy management strategy.

To describe the I-V characteristics of the PV array, a single-diode model is used and shown in Fig. 3.

$$I = N_p\left[I_{ph} - I_s\left\{\exp\left(\frac{q}{AkT}\left(\frac{V}{N_s}+\frac{I}{N_p}R_s\right)\right)-1\right\} - \frac{\frac{V}{N_s}+\frac{1}{N_p}R_s}{R_p}\right] \quad (1)$$

In this equation, I and V respectively, are current and voltage of the PV array, I_{ph} is the current generated by the incident light, I_s is the diode saturation current, T is the cell operating temperature in

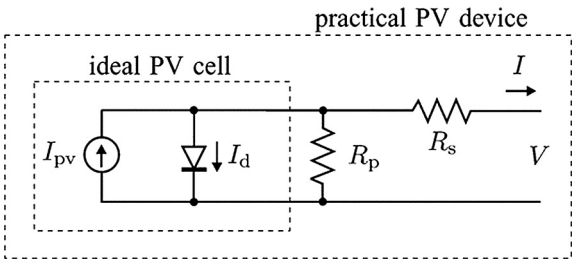

Fig. 3. Single-diode model of the theoretical PV (Villalva et al., 2009).

Kelvin, A is the diode quality factor, Q is the electron charge ($1.6 * 10^{-19}$ C), k is the Boltzmann's constant ($1.38 * 10^{-23}$ J/C), R_s is the series and RP is the parallel resistances of the cell. N_s is the number of cells connected in series and N_p is the number of cell strings that are connected in parallel (Mahmood et al., 2012).

These parameters using a method similar to the method that used in Villalva et al. (2009) have been estimated. However, because the method in Villalva et al. (2009), needs the practical maximum power $P_{max,e}$ for any new non-nominal conditions of temperature and solar radiation to estimate short-circuit current I_{sc}, open circuit voltage V_{oc}, as well as I_{ph} and I_s, so an easier way to use other experimental data was used in the calculations. Here I_s is calculated from the Eq. (2) (Mahmood et al., 2012).

$$I_s = \frac{I_{sc}}{\exp\left(\frac{qV_{oc}}{kTAN_s}\right)-1} \quad (2)$$

Considering the low cost, simplicity and voltage conditions, a unidirectional Boost converter for PV and a bidirectional Buck/Boost converter for the battery are used (Mahmood et al., 2015, 2012, 2014). These converters are shown in Fig. 2.

Lead acid batteries, due to the fact that after the end of their life will be restored again, are the perfect solution for use in the solar system (Lead Acid Battery Guide for Stand Alone Photovoltaic Systems, 1999). So, according to the similar research works and former experiences, the lead-acid battery type is selected in the proposed system (Mahmood et al., 2015, 2012, 2014; Lead Acid Battery Guide for Stand Alone Photovoltaic Systems, 1999).

For simulation and test of the proposed control strategy, a resistive load is used that its value changes for different values of powers.

3. Control system and power management strategy

3.1. Control system

The control system has three parts, including the unidirectional converter controller, bidirectional converter controller and the MPPT algorithm. PI multi loop controllers are used in the system.

In this system, the measured voltage is compared with the reference value initially and generate the reference current. Then the reference current is compared with measured current and the desired duty cycle is achieved.

3.1.1. Unidirectional converter controller

The controller for the unidirectional Boost converter is shown in Fig. 4.

Linear state space equations for a unidirectional Boost converter according to Xiao et al. (2007), are given in Eq. (3).

$$\begin{cases} L_{pv}\frac{di_{L_{pv}}}{dt} = V_{pv} + V_{dc}d \\ C_{pv}\frac{dV_{pv}}{dt} = -i_{L_{pv}} + \frac{V_{pv}}{r_{pv}} \end{cases} \tag{3}$$

r_{pv} is indeed one of the essential characteristics of the PV panels so that its value is determined based on the I-V characteristic curve of the PV panel. The value of this parameter depends on the PV operating point on the I-V characteristic curve and the amount of solar radiation. Also, it has different values for different circumstances ($r_{pv} = -V/I$).

In this equation V_{dc} is the nominal voltage of DC link, which is assumed to be constant, r_{pv} is the dynamic resistance of the PV array (a negative value) around operating point and d is the averaged control input of the system. By using Eq. (3), the transfer function $G_{id\text{-}pv}$ from d to i_{Lpv}, and the transfer function $G_{vi\text{-}pv}$ from i_{Lpv} to V_{pv} are calculated as follows.

$$G_{id-pv}(s) = \frac{i_{L_{pv}}(s)}{d(s)} = \frac{(C_{pv}r_{pv} - 1)V_{dc}}{L_{pv}C_{pv}r_{pv}s^2 - L_{pv}s + r_{pv}} \tag{4}$$

$$G_{vi-pv} = \frac{v_{pv}(s)}{i_{L_{pv}}(s)} = \frac{-r_{pv}}{C_{pv}r_{pv}s - 1} \tag{5}$$

The time constant of the low pass filter (LPF_i) is intended for 10^{-3} s experimentally. According to the approach chosen in reference Mahmood et al. (2012), PI controllers have been calculated and designed by using frequency response of the averaged system and hence by using different values of r_{pv}, at the extrema of the voltage source region ($r_{pv\text{-}vs}$) and current source region ($r_{pv\text{-}cs}$) from the I-V characteristic curve of PV (Fig. 5).

PI controller by using the proposed method in reference Mahmood et al. (2012) has been selected as follows:

$$G_{PI-pv1}(s) = \frac{0.25s + 125}{s} \tag{6}$$

$$G_{PI-pv2}(s) = \frac{0.005s + 20}{s} \tag{7}$$

3.1.2. Bidirectional converter controller

Bidirectional Buck-Boost converter controller for charging mode is shown in Fig. 6.

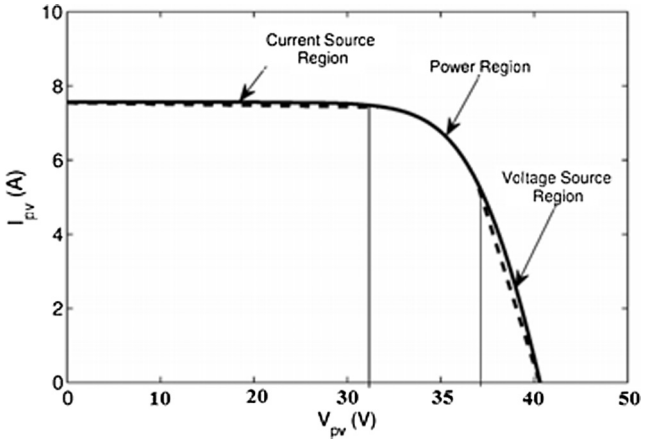

Fig. 5. Operating regions of PV (Mahmood et al., 2012).

The linearized averaged state space equations for bidirectional Buck-Boost converter is as follows (Mahmood et al., 2012, 2014):

$$\begin{cases} L_B\frac{di_B}{dt} = -(1-D)V_{dc} + V_{dc}d \\ C\frac{dV_{dc}}{dt} = (1-D)i_{L_B} - \frac{V_{dc}}{R} - I_{L_B}d \end{cases} \tag{8}$$

In Eq. (8) I_{LB}, D, R, and V_{dc}, are respectively inductor current, duty cycle, equivalent load resistance and DC link voltage at the operating point. The C parameter is the combination of two parallel DC link capacitors, $C_{dc1} + C_{dc2}$. From Eq. (8), the transfer functions $G_{id\text{-}B}(s)$ from the control input d to i_{LB} and $G_{vi\text{-}B}(s)$ from i_{LB} to v_{dc} can be calculated in the form of Eqs. (9) and (10):

$$G_{id-B}(s) = \frac{i_{L_B}(s)}{d(s)} = \frac{RCV_{dc}s + [(1-D)RI_{L_B} + V_{dc}]}{RCL_Bs^2 + L_Bs + R(1-D)^2} \tag{9}$$

$$G_{vi-B}(s) = \frac{v_{dc}(s)}{i_{L_B}(s)} = \frac{-I_{L_B}RL_Bs + V_{dc}R(1-D)}{V_{dc}RCs + [V_{dc} + (1-D)I_{L_B}R]} \tag{10}$$

The time constant of low pass filters LPF_i and LPF_v is selected 10^{-3} s experimentally. The PI controller of the current loop and the voltage loop in the form of Eqs. (11) and (12) have been chosen (Mahmood et al., 2012, 2014):

$$G_{PI-B1}(s) = \frac{0.5s + 125}{s} \tag{11}$$

$$G_{PI-B1}(s) = \frac{0.015s + 15}{s} \tag{12}$$

3.1.3. MPPT algorithm

The implemented algorithm in this system is the incremental conductance (IC) algorithm. IC algorithm is based on dP/dV, which will be zero at the MPP.

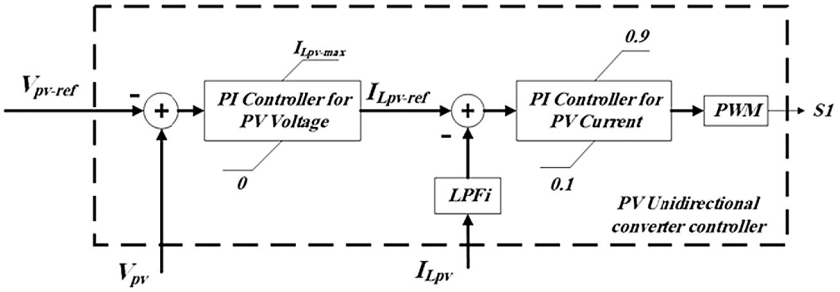

Fig. 4. Unidirectional converter controller for PV (Mahmood et al., 2012).

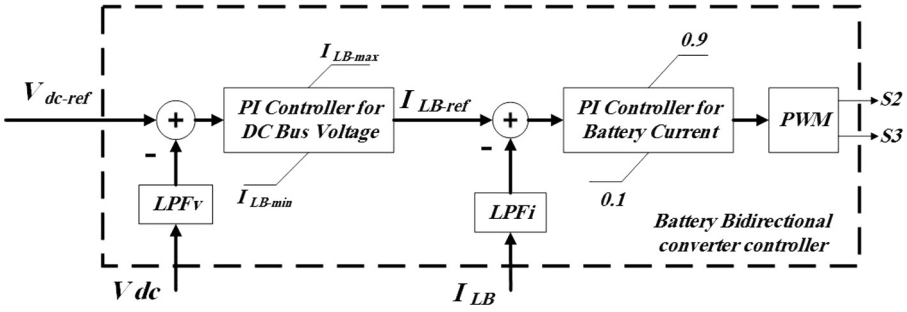

Fig. 6. Bidirectional buck-boost converter controller (Mahmood et al., 2012).

Accordingly, a positive gradient indicates that the operating point is on the left side at the point of MPP, as well as the negative gradient indicates that the operating point is on the right side at the point of MPP.

IC algorithm by measuring V and I in V (t) and I (t) begins the cycle. According to the flowchart of Fig. 7, the MPP can be tracked by comparing the instantaneous conductance (I/V) to the incremental conductance (ΔI/ΔV). The control signal voltage is also adjusted. Based on the output of the comparison above, this variable must be decreased or increased. The MPP is reached once, the V_{ref} is equal to V_{MPP}. At this point the algorithm stops the operation, and this value is stored as long as any changes in the environment are identified a change in ΔI. In this case, the algorithm starts to calculate again to reach the optimal point. The incremental value will determine how fast the algorithm looks for the MPP. Large incremental value helps to decrease the duration of the tracking process. However, the system does not work only at the point of MPP, but oscillates about this point. IC algorithm shows the advantage of better performance under rapidly changing atmospheric conditions. Also, it has is less oscillation around the point of the MPP. However, the efficiency of IC to achieve MPP is almost the same as P&O method. The disadvantage of this method is in partial shade that cannot track the global MPP (Kamarzaman and Tan, 2014).

3.2. The proposed power management strategy

Fig. 8 shows the proposed power management strategy variables. Power flow in the system can be classified into five different scenarios of operation.

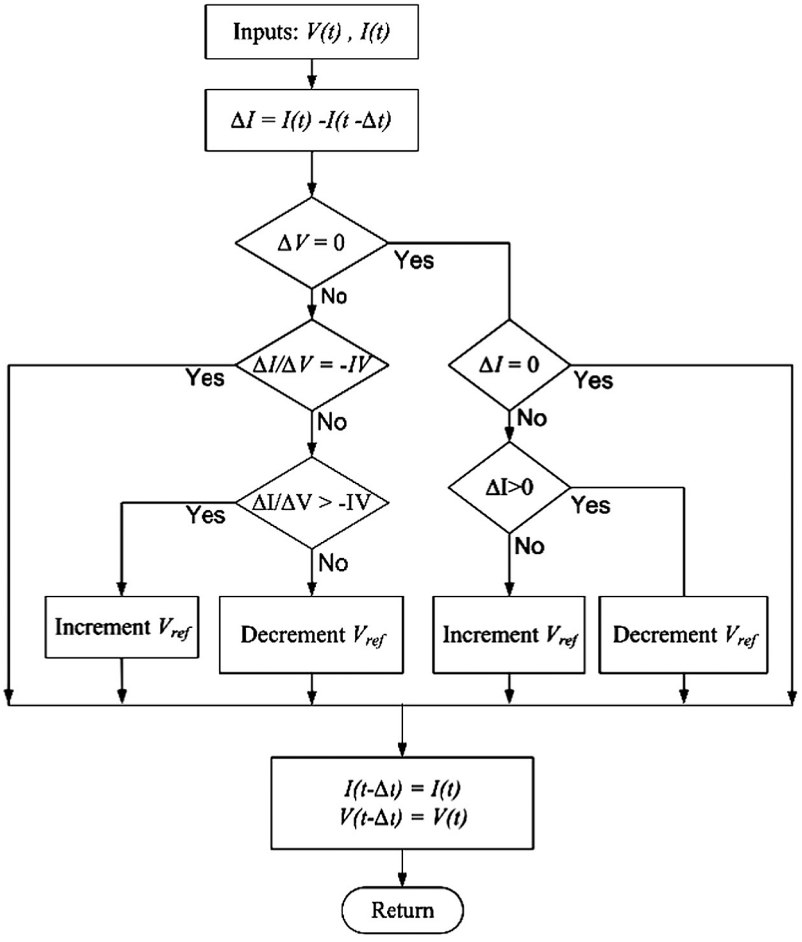

Fig. 7. Flowchart of the incremental conductance MPPT algorithm (Kamarzaman and Tan, 2014).

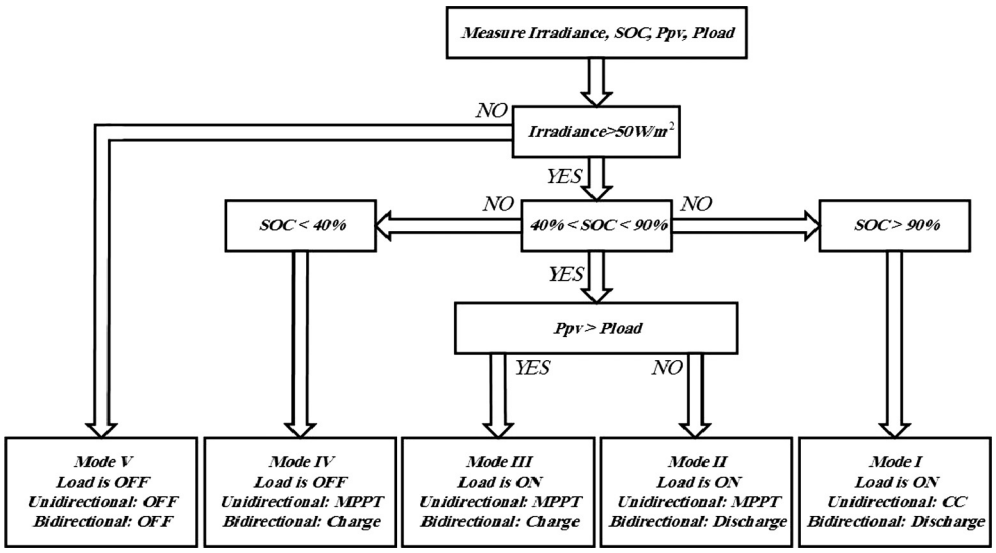

Fig. 8. The proposed power management strategy.

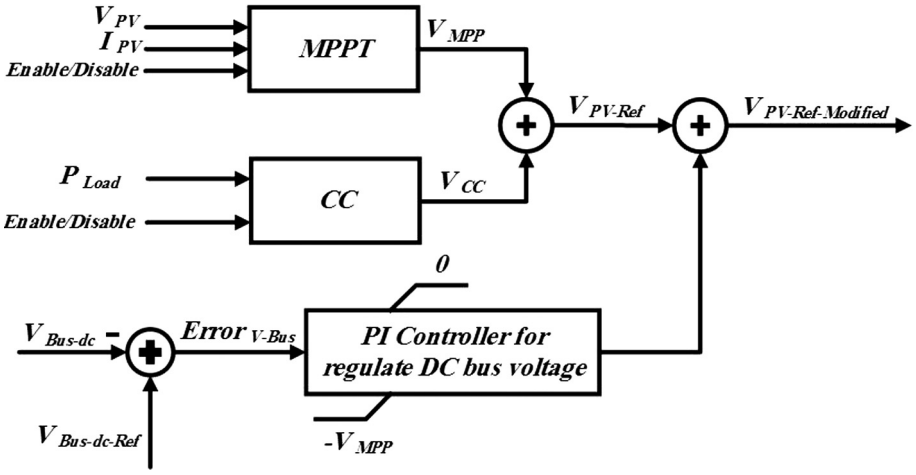

Fig. 9. The PV voltage reference.

Fig. 8 shows that the PV converter can operate in the MPPT mode, in the constant current (CC) mode or in the off mode.

The PV voltage reference is generated by the control block as shown in Fig. 9.

As Fig. 9 shown, if the system (based on the SOC and the amount of the sunlight) requires that the PV converter operates in the MPPT mode, the MPPT block in Fig. 8 is activated through energy management strategy and the CC block is disabled. So, the PV reference voltage is the MPPT voltage. On the other hand, if the system (based on the SOC and the amount of the sunlight) requires that the PV converter operates in the CC mode, the MPPT block is disabled and the CC block is enabled. As a result, the PV reference voltage is the CC voltage. Also, this voltage is less than the MPP voltage because the PV operating point enters into the constant current area. The CC voltage is determined according to the load required power. In this case, the output load is modeled as a pure resistive load and its value is determined by calculating the output voltage and the output current. But in practical terms, there are capacitive and inductive loads. So, the desired voltage is not accurate enough. Consequently, the value of the voltage is modified by the PI controller to regulate the DC bus voltage (overvoltage or voltage drop conditions do not happen).

It should be noted that, Activation and deactivation pulses in Fig. 9 are generated by a power management strategy of Fig. 8. The PI controller which controls the DC bus voltage helps that when the load is too low or when the battery charging current is greater than the capacity of the battery charging current, overvoltage on the DC bus will not occur. Then each of the five cases of power management strategy will be described in the following.

Mode1: This mode occurs when the SOC of the battery reaches to 90 percent. Since the battery is charged only on condition that the power generated by PV is more than the power required of load, consequently, when the SOC of the battery reaches to 90 percent (the battery is fully charged) the PV power is greater than the power required by the load. In this case, the battery should not continue to charge and returns to the discharge mode. It is noteworthy that, because the battery is always responsible for regulating the DC link voltage, the battery cannot be disconnected in this condition. Although, this discharge mode will be set in a way that a very low current around 0.1 A drawn from the battery. Now that the battery cannot be charged, the additional power that produces by solar panel will cause an overvoltage in the DC link. To avoid this over voltage, generated power by PV should be decreased. Slight change in the PV voltage will move the PV far from MPP to

Table 1
Key parameters of the entire PV/battery system.

Value	Parameter	Character
100 μF	C_{PV}	Input capacitor in PV system
600 μH	L_{PV}	Inductor in PV system
100 μF	C_{DC1},C_{DC2}	Output capacitors
500 μH	L_B	Inductor in the battery system
100 V	$V_{DC\text{-}ref}$	Nominal voltage of DC link
24 V	V_B	Nominal voltage of battery
41.8 V	V_{OC}	Open circuit voltage of PV array
33.9 V	V_{MMP}	MPP voltage for PV
7.13 A	I_{SC}	Short circuit current of PV array
50 Ω, 100 Ω	R	Loads

reach this goal. It should be noted that in practice as soon as the SOC of the battery reaches 90 percent, bidirectional and unidirectional converters respectively from charging mode and MPPT go to the discharging mode and CC. However, to avoid frequent change in converters modes between these two modes, back them done with little delay. For example, as long as the SOC of the battery has not reached to 80%, the system is not allowed to return to its previous mode. In fact, the comparison between SOC of the battery with 90 percent is done through the hysteresis comparator. Because of the low current that can be drawn from the battery, the duration will be longer and the system will experience a suitable stable condition.

Mode 2: This mode occurs when the SOC of the battery is in the normal condition (between 40 and 90 percent), and the power generated by PV is less than the load power. In this case, only the PV cannot feed the load, so the battery also helps it. In this situation, the battery converter is in discharging mode, PV converter is in the MPPT mode and the load is connected.

Mode 3: This mode occurs when the SOC of the battery is in the normal condition (between 40 and 90 percent), and the power generated by PV is more than the load power. In this case, only the PV feed the load, and the remaining power is used to charge the battery. In this situation, the battery converter is in charging mode, PV converter is in the MPPT mode and the load is connected.

Mode 4: This mode occurs when the SOC of the battery is less than 40% and the power generated by the PV compare to the minimum power, which is a small fixed value, is higher. In this case, because the PV power is less than the load required power and the battery is fully discharged and cannot helps the PV, so the DC link voltage is dropped and in these circumstances the load must be disconnected. Because PV can still generate the power, so the PV power can charge the battery after the load is disconnected. As a result, the PV converter continues to operate in the MPPT mode and the battery converter continues to charge it, while the load is disconnected. In this power management strategy, when the SOC of the battery reaches 40%, the load immediately be disconnected and the battery start charging. However, when the SOC of the battery reaches more than 40% and the load immediately be connected, the system starts to frequent connect and disconnect and the SOC of the battery oscillates around 40%. To prevent of frequent load connect and disconnect condition, after the load was disconnected, back to the load connected mode is

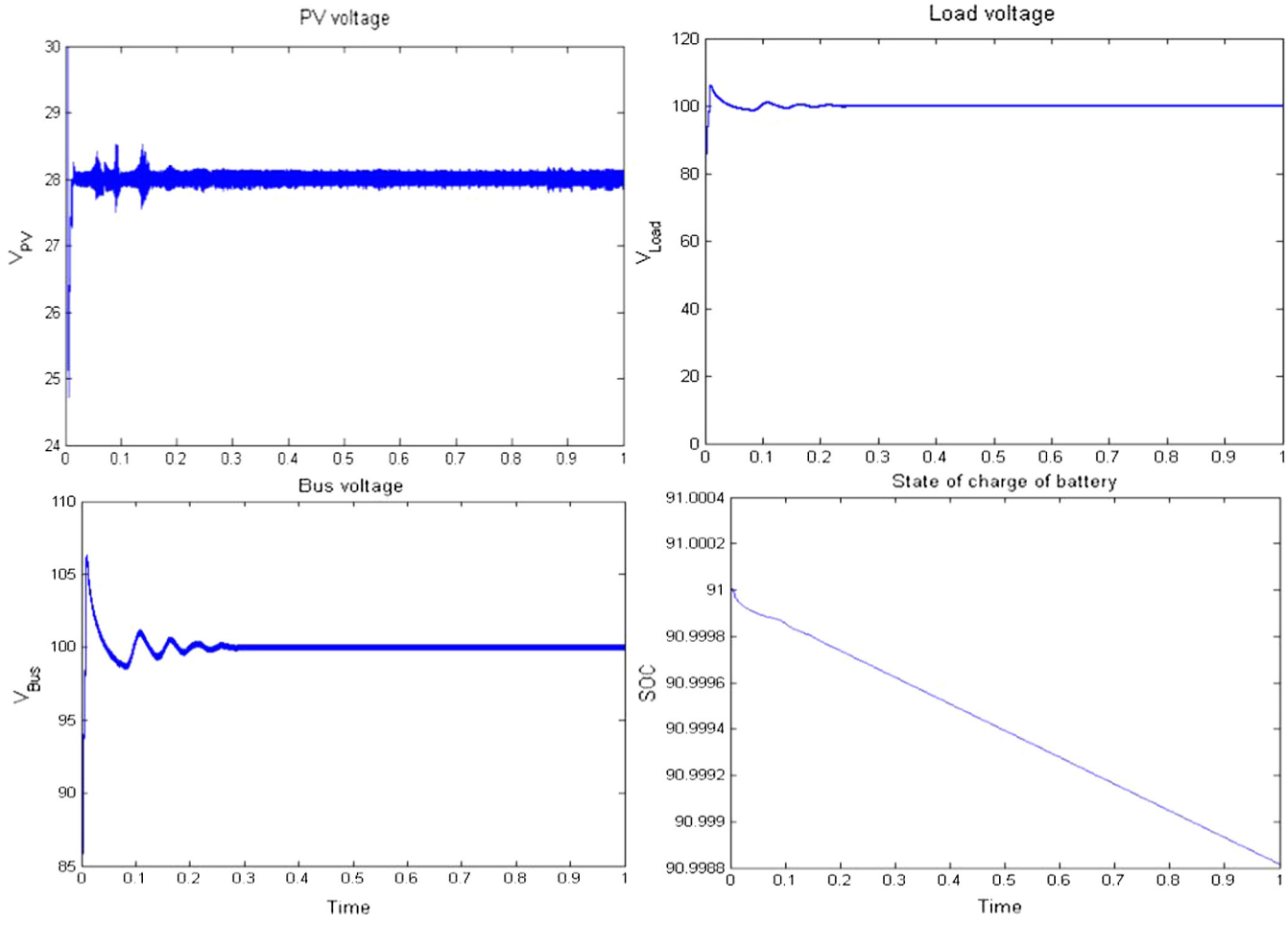

Fig. 10. Operations in mode 1; the PV voltage, the load voltage, the DC bus voltage and the SOC of battery.

done with some delay to ensure that the system has reached the steady state of power generation. To ensure, the battery will be allowed to charge to a certain value (e.g. 70%), then the load is connected. In fact, the comparison between the SOC of the battery with the 40 percent is done through the hysteresis comparator. This will prevent the frequent load connect and disconnect.

Mode 5: This condition occurs when the sunlight radiation is very low or no radiation at all. In this case the system goes into complete off mode until the sunlight radiation starts again.

4. Results

4.1. Simulation results

The simulation is done by using solar panel Sanyo HIP-225HDEI, 225 W. The results is done by Matlab/Simulink software. In Eq. (2) from reference Villalva et al. (2009), the nominal values $I_{sc,n}$ and $V_{oc,n}$ have been replaced with experimental values I_{sc} and V_{oc} for the calculation of I_s in existing working conditions instead of $I_{s,n}$. In each operating point seems to be that I_{ph} is equal to I_{sc}, Because R_s compared to R_p is usually very small. R_s and R_p by matching the calculated P_{max} with experimental $P_{max,e}$ for each experimental condition is calculated. To achieve the best experimental results, the diode quality factor is considered 1.5. Here, each panel contains 60 cells in series. The PV array consists of one string. Thus, for this structure N_s is $60 * 1$ and the N_p, is equal to 1.

In the proposed system the lead-acid battery type is selected. The capacity of the battery should be sized so that it can be full charge during the day and be ready to feed a load of 200-W in the absence of the sunlight radiation. Medium time for charging the battery is about 5–10 h (Lead Acid Battery Guide for Stand Alone Photovoltaic Systems, 1999). To do so a battery with a capacity of 80 A h is chosen.

Key parameters of the entire PV/battery system that has been introduced in the previous sections are shown in Table 1.

A resistive load is used to evaluate the system performance in the high-load and low-load modes. 50 Ω resistance at high load mode (200 W) and 100 Ω resistance at the low load mode (100 W) have been considered.

4.1.1. Simulation of each modes

In this section, the simulation is done for testing the performance of control system in different modes of energy management strategies according to Fig. 8 individually.

These strange behaviors at the beginning are due to simulation because the simulation is done with all devices connected simultaneously at first. But these conditions do not occur in the real world where the devices connect together one by one in the synchronous and controlled mode for minimizing the transient states.

Mode 1: It is assumed that the sunlight radiation is 975 W per square meter and in this case, the SOC of the battery is more than 90 percent, for example, it is 91% and the load is 200 W.

If these conditions occur, energy management system, change the system's operating mode to the mode 1. In the mode 1, load is connected. The input voltage of unidirectional converter is in the CC mode and bidirectional converter is in discharging mode.

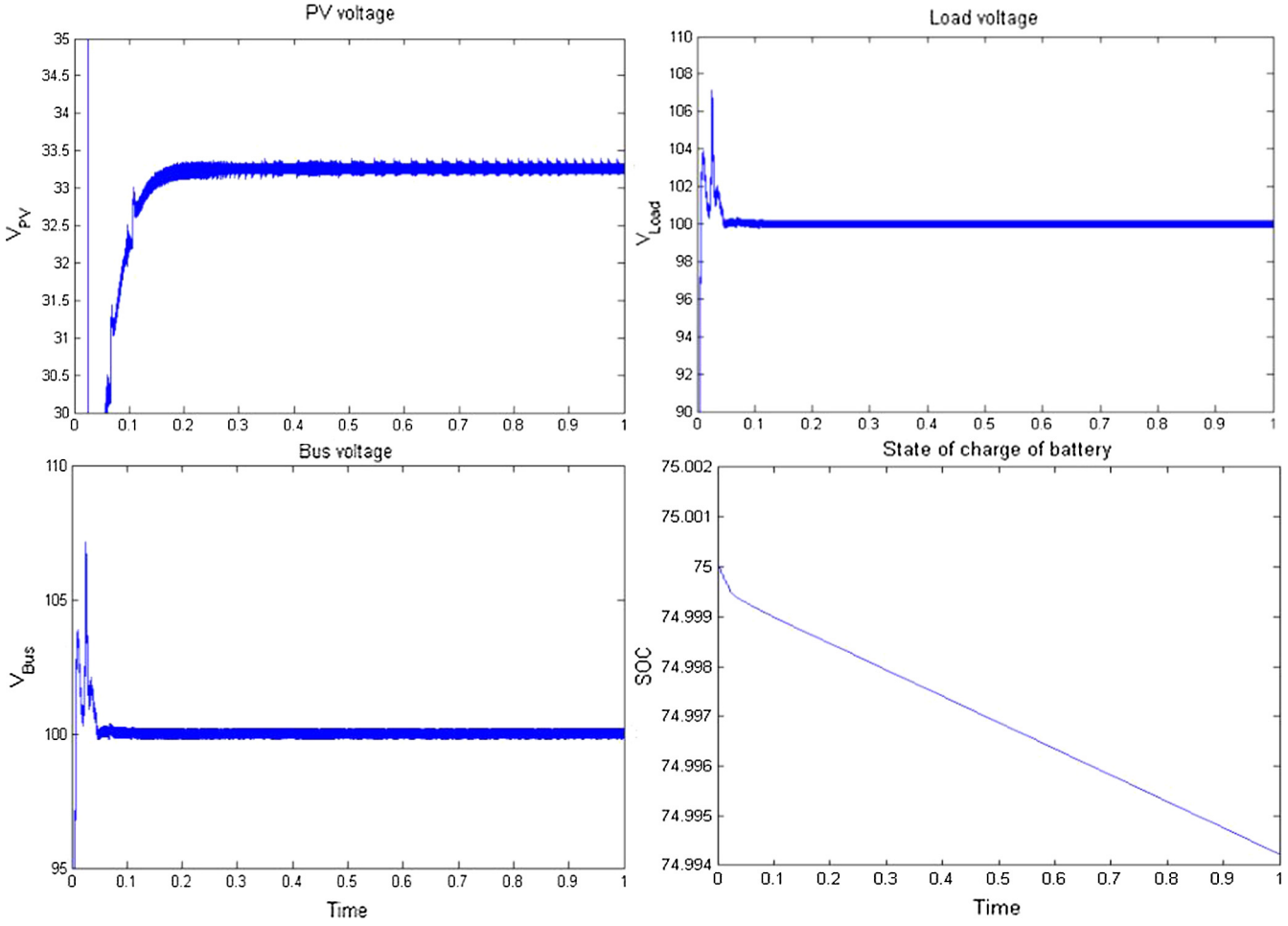

Fig. 11. Operations in mode 2; the PV voltage, the load voltage, the DC bus voltage and the SOC of battery.

In Fig. 10, the PV voltage, the load voltage, the DC bus voltage and the SOC of battery can be seen in the first mode.

Mode 2: It is assumed that the sunlight radiation is 700 W per square meter and in this case, the SOC of the battery is less than 90 percent, for example, it is 75% and the load is 200 W.

If these conditions occur, system power management takes the system's operating mode to the mode 2. In this mode, the load is connected. This is due to the radiation conditions and the state of SOC (according to energy management strategies in Fig. 8). The unidirectional converter of PV works in the MPPT mode and the bidirectional converter of battery works in the discharging mode. In Fig. 11, the PV voltage, the load voltage, the DC bus voltage and the SOC of the battery can be seen in the second mode.

Mode 3: It is assumed that the sunlight radiation is 975 W per square meter and in this case, the SOC of the battery is less than 90 percent, for example, it is 75% and the load is 200 W.

If these conditions occur, system power management, take the system's operating mode to the mode 3. In this mode, the load is connected. The unidirectional converter of PV works in the MPPT mode and the bidirectional converter of battery works in the charging mode. In Fig. 12, the PV voltage, the load voltage, the DC bus voltage and the SOC of the battery can be seen in the third mode.

Mode 4: It is assumed that the sunlight radiation is 500 W per square meter and in this case, the SOC of the battery is less than 40 percent, for example, it is 30% and the load is 200 W.

If these conditions occur, system power management, take the system's operating mode to the mode 4. In this case, because the battery is fully discharged and the PV cannot feed the load, so the load is disconnected. The unidirectional converter of PV works in the MPPT mode and the bidirectional converter of the battery works in the charging mode. In Fig. 13, the PV voltage, the load voltage, the DC bus voltage and the SOC of the battery can be seen in the fourth mode.

Mode 5: If the sunlight radiation is less than 50 W per square meter, system power management, take the system's operating mode to the mode 5. In the fifth mode, converters turned off. Also, according to the radiation conditions and the state of SOC (according to energy management strategies in Fig. 8) the load is disconnected.

4.1.2. The transition of PV converter operation from MPPT to CC mode

As Fig. 8 (energy management strategy) shows, for example, in the first mode the PV converter is in the CC mode and in the second, third and fourth is in the MPPT mode. So just a change of state occurs from MPPT to CC mode (mode 1 to mode 2). Moreover, only one transition of the battery converter from charging to discharging mode and only one transition of load from connecting to disconnecting mode occurs according to the energy management strategy in Fig. 8 that are explained in Sections 4.1.2–4.1.4 respectively.

If the SOC of the battery value close to 90 percent, for example, is 89.95 percent, the sunlight radiation is 975 W per square meter and the system is being fed a load of 100 W, after a while that the circuit operated in the charging mode, the SOC of the battery reaches 90 percent. In this condition, the state of the PV converter

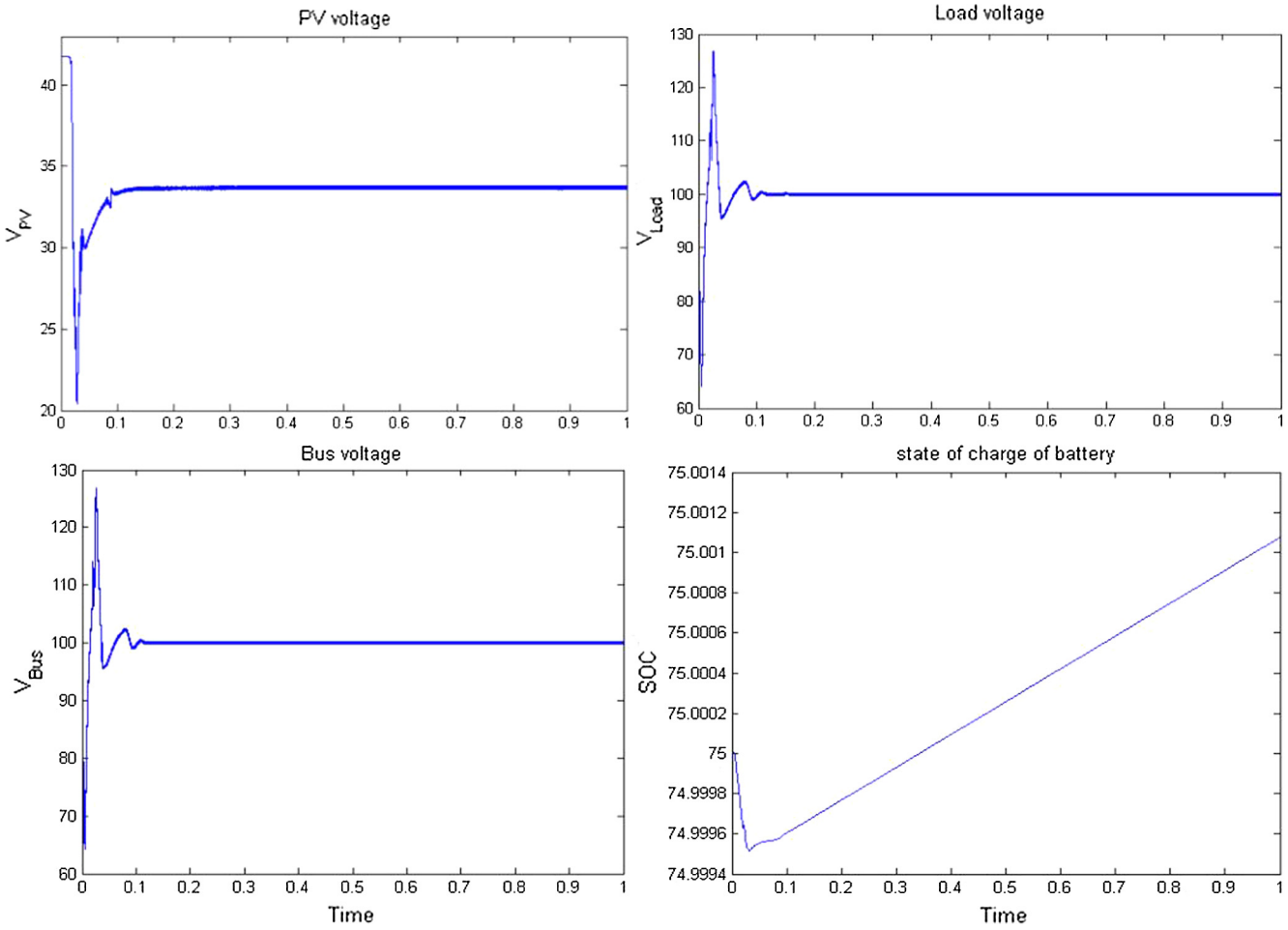

Fig. 12. Operations in mode 3; the PV voltage, the load voltage, the DC bus voltage and the SOC of battery.

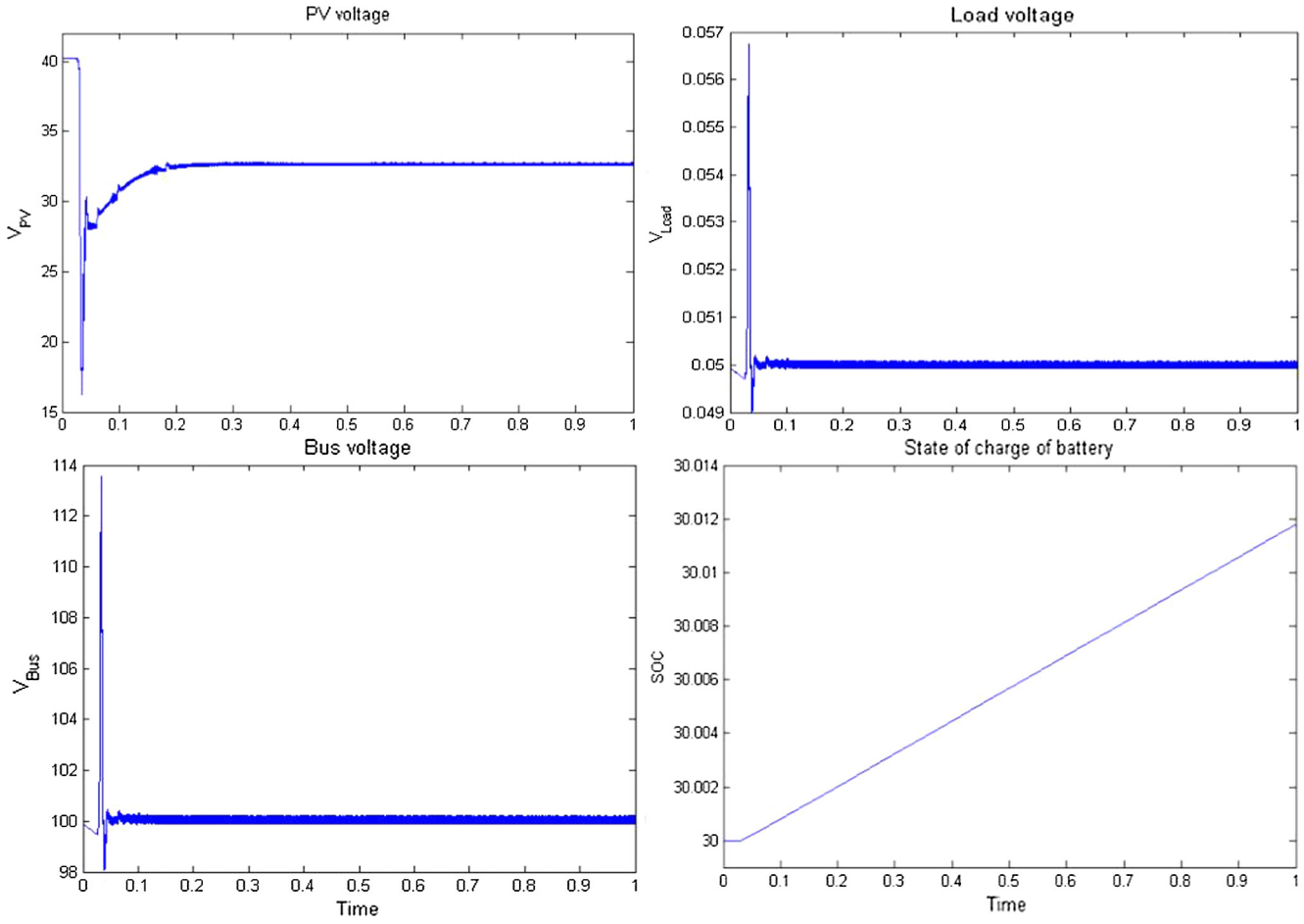

Fig. 13. Operations in mode 4; the PV voltage, the load voltage, the DC bus voltage and the SOC of battery.

operation changes from MPPT to CC Mode. The PV and the DC bus voltage in this condition are depicted in Fig. 14.

4.1.3. The transition of battery converter from charging to discharging mode

It is assumed that the SOC of the battery is 75% and the sunlight radiation varies from 975 W per square meter to 700 W per square meter. So that at the beginning the PV power is more than the load power and at the end, the PV power is less than the load power. Anyway, the system is being fed a load of 200 W.

In this case, after a while that the bidirectional converter worked in charging mode, by reducing the sunlight radiation it will be transferred to the discharging mode. In these two cases, PV must operate in MPPT mode and its output power reduces propor-

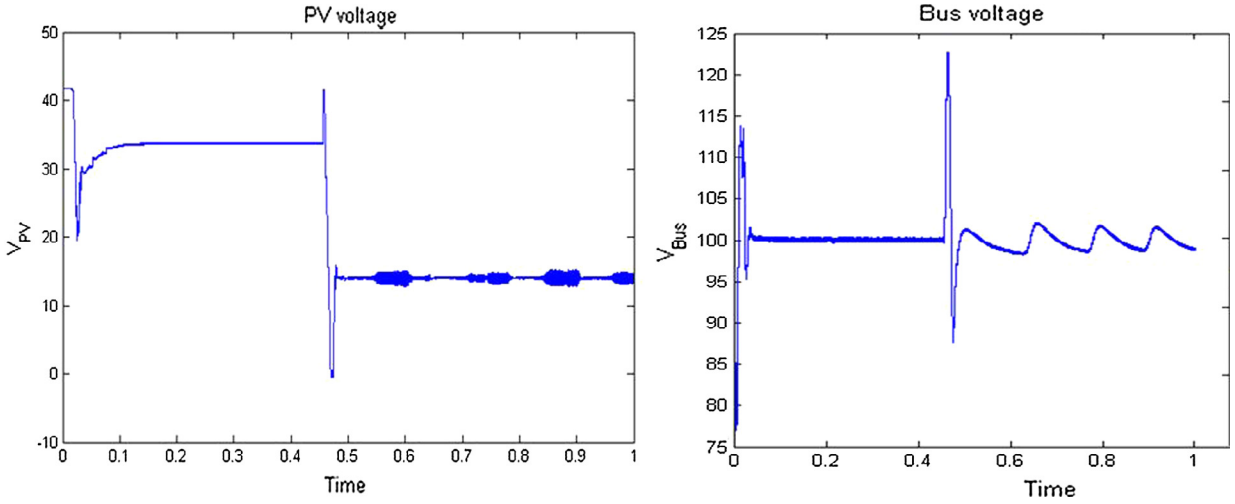

Fig. 14. The PV voltage and the DC bus voltage in transition from MPPT to CC.

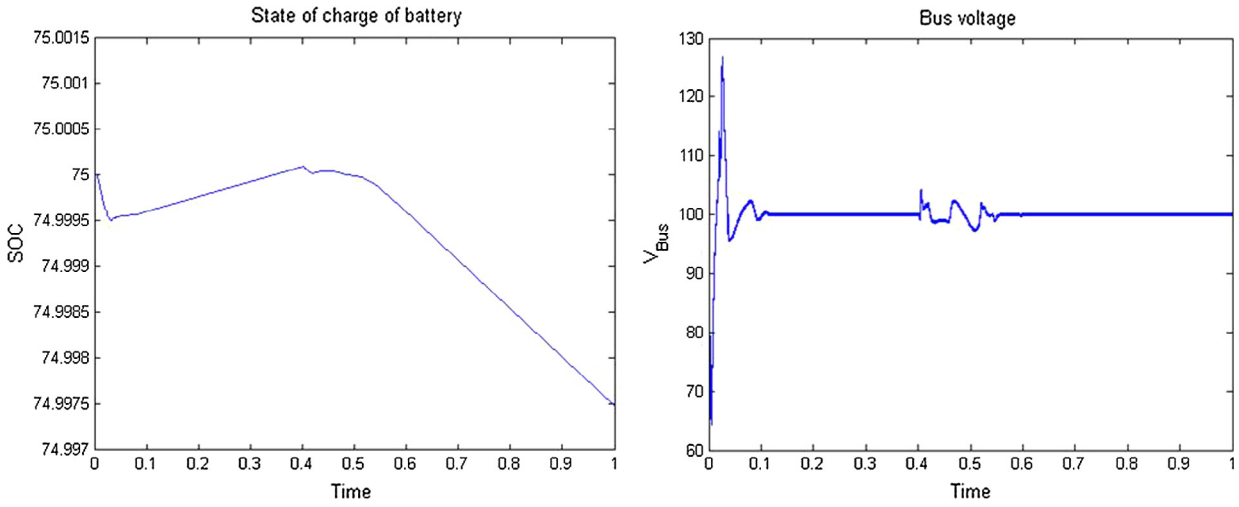

Fig. 15. SOC and the DC bus voltage in transition from charging to discharging mode.

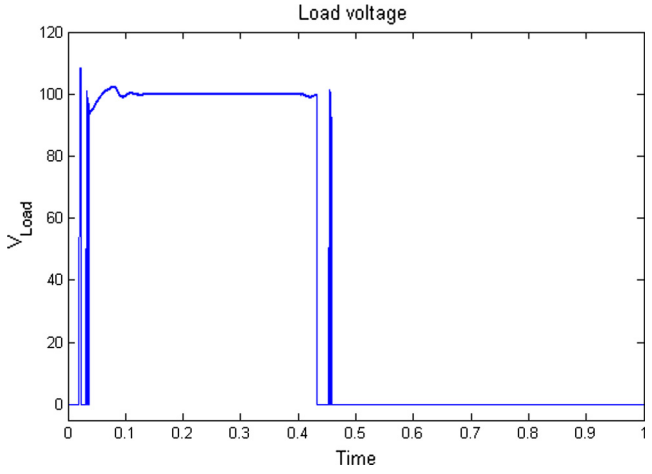

Fig. 16. The load voltage in transition from connecting to disconnecting mode.

tionally with decreasing of the sunlight irradiance. In Fig. 15 the battery charging mode and the DC bus voltage in the transition state is observed.

4.1.4. The transition of load from connecting to disconnecting mode

It is assumed that the SOC of the battery is less than 40% and the sunlight radiation varies from 975 W per square meter to 700 W per square meter. So that at the beginning, the PV power is more than the load power and at the end, the PV power is less than the load power. Also, the system is being fed a load of 200 W.

After a while that the bidirectional converter worked in charging mode, by reducing the sunlight irradiance, the PV power will become less than the required power. The load voltage situation can be seen in Fig. 16. The fast peak voltages in Fig. 16 are transient behaviors from connecting to disconnecting mode. In fact, this property is the natural behavior of switching (Havanur, 2008).

4.2. Experimental results

Final setup of the system is shown in Fig. 17. The system is controlled by DSP TMS320F2812 Starter Kit IDC2812DSKv2. PCB board is designed by using Altium Designer software. According to the capacities needed, IRFP264 and IRFP260 power MOSFETs are selected experimentally as power switches in the proposed system. Voltage measurements are done by using a resistive voltage divider and current measurements are done by applying the ACS712 current sensor. Due to hardware limitations, a fixed resistor load is used to simulate the load of the system and its value is 45 Ω.

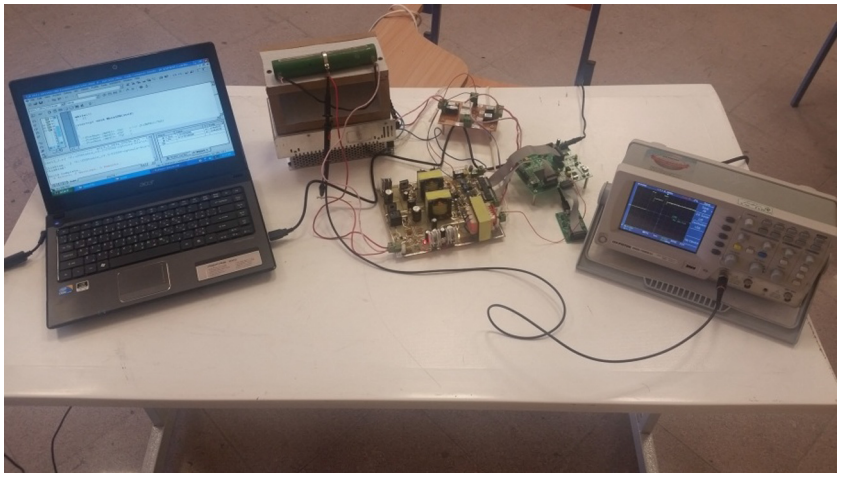

Fig. 17. Final setup of the system.

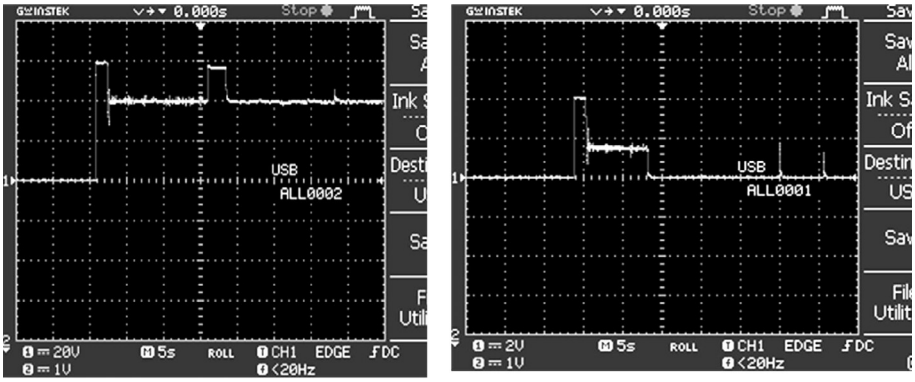

Fig. 18. (a) The DC bus voltage in reference voltage of 40 V and load resistance of 45 Ω, (b) The battery current in reference voltage of 40 V and load resistance of 45 Ω.

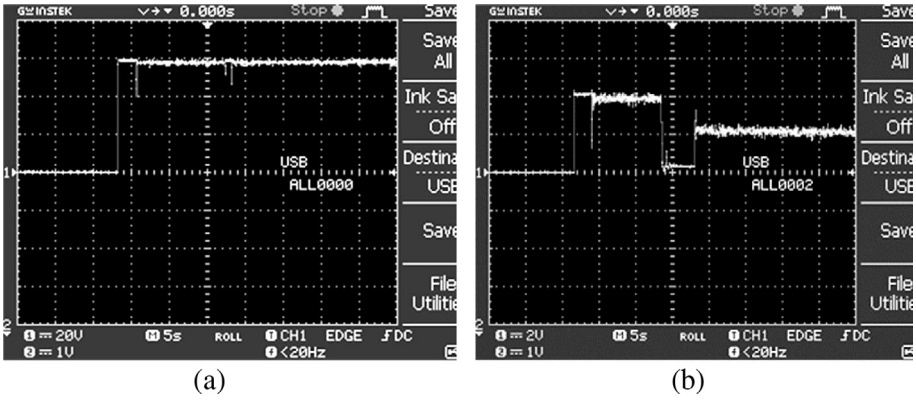

Fig. 19. (a) The DC bus voltage in reference voltage of 60 V and the load resistance of 45 Ω, (b) the battery current in reference voltage of 60 V and the load resistance of 45 Ω.

Experimental results are shown in the following sections. To show the flexibility of control system, the circuit has been tested in two different situations.

4.2.1. The test 1 (power transmission of 36 W)

In the first experiment, the DC bus reference voltage is set at 40-V. In this case, the load resistance is 45 Ω. Also, the output power is 36 W and the PV can feed the load alone. The DC bus voltage waveform and the battery current waveform are shown in Fig. 18a and b respectively.

As Fig. 18 shows, in the beginning that PV is not yet connected, the total load current is supplied by the battery. Then, when the PV connected (it can supply the total load), the battery output current reaches to almost zero and the battery only regulates the DC bus voltage. The two peaks in DC bus voltage respectively represent the moments of connecting the PV and the battery to the circuit at the start of system operation where the battery is not fully charged. After that, the control system works properly and the voltage becomes stable.

4.2.2. The test 2 (power transmission of 80 W)

In the second experiment, the DC bus reference voltage is set at 60-V. In this case, the load resistance is 45 Ω. Also, the output power is 80 W and the PV cannot fed the load alone. The DC bus voltage waveform and the battery current waveform are shown in Fig. 19a and b respectively.

As Fig. 19 shows, in the beginning that PV is not yet connected, the total load current is supplied by the battery. Then, when the PV connected (it cannot supply the total load), so the battery output current reaches to almost 2 A.

5. Conclusion

In this paper, a new control strategy and power management for a stand-alone PV/battery hybrid power system has been suggested. The solar cell arrays provide energy in the steady-state and the battery provides energy in transient states. Here, a charge controller system based on the MPP tracking technology, suitable for using in the islanded micro grid that contains a solar panel and a battery is designed. The charge controller includes a unidirectional DC-DC converter as an interface circuit between the solar panel and the DC bus, a bidirectional DC-DC converter as an interface circuit between the battery and the DC bus with a control system and power management in different states of irradiance and the SOC. A 200-W prototype system is designed and simulated. The simulation and experimental results are showing the best performance of the proposed charge controller in different conditions.

References

Chiang, S.J., Shieh, H.J., Chen, M.C., 2009. Modeling and control of PV charger system with SEPIC converter. IEEE Trans. Industr. Electron. 56, 4344–4353.
Fathabadi, H., 2016. Novel high efficiency DC/DC boost converter for using in PV systems. Sol. Energy 125, 22–31.
Fernão Pires, V., Foito, D., Baptista, F.R.B., Fernando Silva, J., 2016. A PV generator system with a DC/DC converter based on an integrated Boost-Ćuk topology. Sol. Energy 136, 1–9.

Hasan, K.N., Haque, M.E., Negnevitsky, M., Muttaqi, K.M., 2009. Control of energy storage interface with a bidirectional converter for PV systems. In: Power Engineering Conference, 2008. AUPEC '08. Australasian Universities, pp. 1–6.
Havanur, S., 2008. Quasi-clamped inductive switching behavior of power Mosfets. In: Power Electronics Specialists Conference, PESC 2008. IEEE, pp. 1–5.
Kamarzaman, N.A., Tan, C.W., 2014. A comprehensive review of MPP tracking algorithms for PV systems. Renew. Sustain. Energy Rev. 37, 585–598.
Karami, N., Moubayed, N., Outbib, R., 2012. Analysis and implementation of an adaptative PV based battery floating charger. Sol. Energy 86, 2383–2396.
Lead Acid Battery Guide for Stand Alone Photovoltaic Systems. International Energy Agency, PVPS Task III, 1999, pp. 1–33.
Lu, D.D.C., Nguyen, Q.N., 2012. A PV panel emulator using a buck-boost DC/DC converter and a low cost micro-controller. Sol. Energy 86, 1477–1484.
Mahmood, H., Michaelson, D., Jin, J., 2012. Control strategy for a stand-alone PV/battery hybrid system. In: IECON 2012–38th Annual Conference on IEEE Industrial Electronics Society, pp. 3412–3418.
Mahmood, H., Michaelson, D., Jiang, J., 2014. A power management strategy for PV/battery hybrid systems in islanded microgrids. IEEE J. Emerging Selected Topics Power Electron. 2, 870–882.
Mahmood, H., Michaelson, D., Jin, J., 2015. Decentralized power management of a PV/battery hybrid unit in a droop-controlled islanded microgrid. Power Electron., IEEE Trans. 30, 7215–7229.
Masheleni, H., Carelse, X.F., 1997. Microcontroller-based charge controller for stand-alone PV systems. Sol. Energy 61, 225–230.
Mirzaei, A., Jusoh, A., Salam, Z., Adib, E., Farzanehfard, H., 2011a. Analysis and design of a high efficiency bidirectional DC–DC converter for battery and ultracapacitor applications. Simul. Model. Pract. Theory 19, 1651–1667.
Mirzaei, A., Jusoh, A., Salam, Z., Adib, E., Farzanehfard, H., 2011b. A fully soft switched two quadrant bidirectional soft switching converter for ultra capacitor interface circuits. J. Power Electron. 11, 1–9.
Mojallizadeh, M.R., Badamchizadeh, M., Khanmohammadi, S., Sabahi, M., 2016. Designing a new robust sliding mode controller for MPP tracking of PV cells. Sol. Energy 132, 538–546.
Nguyen, T.-T., Kim, H.W., Lee, G.H., Choi, W., 2013. Design and implementation of the low cost and fast solar charger with the rooftop PV array of the vehicle. Sol. Energy 96, 83–95.
Tofighi, A., Kalantar, M., 2011. Power management of PV/battery hybrid power source via passivity-based control. Renewable Energy 36, 2440–2450.
Villalva, M.G., Gazoli, J.R., Filho, E.R., 2009. Comprehensive approach to modeling and simulation of PV arrays. Power Electron., IEEE Trans. 24, 1198–1208.
Xiao, W., Dunford, W.G., Palmer, P.R., Capel, A., 2007. Regulation of PV voltage. IEEE Trans. Industr. Electron. 54, 1365–1374.
Zhenhua, J., 2006. Power management of hybrid PV - fuel cell power systems. In: 2006 IEEE Power Engineering Society General Meeting, pp. 6–11.
Zhenhua, J., Dougal, R.A., 2004. Multiobjective MPPT/charging controller for stand-alone PV power systems under different insolation and load conditions. In: Industry Applications Conference, 2004. 39th IAS Annual Meeting. Conference Record of the 2004 IEEE, pp. 1154–1160. vol. 2.
Zhiling, L., Xinbo, R., 2009. A novel power management control strategy for stand-alone PV power system. In: Power Electronics and Motion Control Conference, 2009. IPEMC '09. IEEE 6th International, pp. 445–449.